

1 **Biofilm formation by marine bacteria is impacted by**
2 **concentration and surface functionalization of polystyrene**
3 **nanoparticles in a species-specific manner**
4

5 Mira Okshevsky¹, Eva Gautier¹, Jeffrey M. Farner¹, Lars Schreiber², Nathalie Tufenkji^{1*}

6 ¹ Department of Chemical Engineering, McGill University, Montreal, Canada

7 ² Energy Mining and Environment Research Center, National Research Council of Canada,
8 Montreal, Canada

9 *corresponding author

10

11 **Originality-Significance Statement**

12 This work provides the first experimental evidence of how biofilm formation by marine bacteria
13 is impacted by polystyrene nanoplastics and demonstrates that surface charge and concentration
14 play important roles. The results of this study are significant to the scientific community, as they
15 demonstrate the concentrations at which nanoplastics impact biofilm formation of marine
16 bacteria.

17 **Summary**

18 The world's oceans are becoming increasingly polluted by plastic waste. In the marine
19 environment, larger plastic pieces degrade into nanoscale (<100 nm in at least one dimension)
20 plastic particles due to natural weathering effects. We observe that the presence of 20 nm plastic
21 nanoparticles at concentrations below 200 ppm had no impact on planktonic growth of a panel of
22 heterotrophic marine bacteria. However, the presence of plastic nanoparticles significantly
23 impacted the formation of biofilms in a species-specific manner. While carboxylated
24 nanoparticles increased the amount of biofilm formed by several species, amidine-functionalized
25 nanoparticles decreased the amount of biofilm of many but not all bacteria. Further experiments
26 suggested that the aggregation dynamics of bacteria and nanoparticles were strongly impacted by
27 the surface properties of the nanoparticles. The community structure of an artificially constructed
28 community of marine bacteria was significantly altered by exposure to plastic nanoparticles, with
29 differently functionalized nanoparticles selecting for unique and reproducible community
30 abundance patterns. These results suggest that surface properties and concentration of plastic
31 nanoparticles, as well as species interactions, are important factors determining how plastic
32 nanoparticles impact biofilm formation by marine bacteria.

33 **Introduction**

34 Marine environments are becoming increasingly polluted by plastics. By the year 2025, it is
35 estimated that the oceans will contain more than 25 Mt of plastic litter (Jambeck et al., 2015).

36 Research into the environmental impacts of plastic litter has predominately focused on plastics at
37 the macro (>5 mm) and micro (<5 mm) scales. Concentrations of these plastics in the marine
38 environment vary widely (Auta, Emenike, & Fauziah, 2017), with one study calculating that over
39 a period of three days, more than two billion macro and microplastics entered coastal waters
40 from two southern Californian rivers alone (Moore, Lattin, & Zellers, 2011). The fragmentation
41 of microplastics into nanoplastics (<100 nm in at least one dimension) is anticipated in marine
42 environments (Andrady, 2011), with studies confirming the presence of submicron plastic
43 particles in ocean water beginning to emerge together with advances in detection technology
44 (Ter Halle et al., 2017). In the marine environment, natural weathering effects caused by sand
45 abrasion, waves and UV radiation (Gigault, Pedrono, Maxit, & Ter Halle, 2016), as well as
46 digestive fragmentation (Dawson et al., 2018) degrade plastic waste into plastic nanoparticles.

47 The process of larger plastic pieces degrading into the nanoscale has been observed in simulated
48 weathering conditions (Lambert & Wagner, 2016; Shim et al., 2014). Placed in a weathering
49 chamber, 1 cm² coupons from the polystyrene lids of disposable coffee cups released billions of
50 submicron particles to the surrounding liquid within two months (Lambert & Wagner, 2016).

51 Similarly, a recent report looking at nylon and polyethylene terephthalate teabags steeped in 95
52 °C water for 5 min observed the formation of billions of micro and nanoplastics (Hernandez et
53 al., 2019). Degraded microplastics are associated with surface defects such as microcrack
54 formation and bubbling or pitting, while the generated nanoplastics are frequently close to
55 spherical in shape (Cooper & Corcoran, 2010; Corcoran, Biesinger, & Grifi, 2009; Hernandez et

56 al., 2019; Hüffer, Weniger, & Hofmann, 2018; Lambert & Wagner, 2016; Yousif & Haddad,
57 2013). The formation of nanoplastics in simulated marine environments has been shown to lead
58 to the formation of fractal aggregates, and critical coagulation constants are often observed in the
59 order of $10^{-3} - 10^{-2}$ M and $10^{-2} - 10^{-1}$ for multivalent and monovalent salts, respectively (Alimi,
60 Farner Budarz, Hernandez, & Tufenkji, 2018; Gigault et al., 2016; Koelmans, Besseling, &
61 Shim, 2015). This suggests that nanoplastics will readily aggregate in marine environments, with
62 this aggregation expected to depend on surface charge and the presence of coatings, such as
63 exopolymeric substances produced by bacteria (Alimi et al., 2018; Summers, Henry, &
64 Gutierrez, 2018).

65
66 Despite evidence that the oceans are becoming contaminated with small plastic particles, very
67 few studies have examined the ecological impact of nanoscale plastic waste on marine
68 organisms. The majority of studies that do exist, focus on macroorganisms such as mussels
69 (*Mytilus edulis*) and oysters (*Crassostrea virginica*), which have been shown to take up 100 nm
70 polystyrene beads (Ward & Kach, 2009). Recently, the commercially important mollusc *Pecten*
71 *maximus* was shown to uptake polystyrene nanoparticles at environmental concentrations of less
72 than 0.015 ppm (Al-Sid-Cheikh et al., 2018).

73
74 Studies conducted to date on the impact of plastic nanoparticles on marine microorganisms have
75 largely focused on photosynthetic microorganisms. For example, it has been shown that
76 polystyrene nanoparticles modified with carboxyl groups (carboxyl nanoparticles; CNP) attach
77 onto the surface of microalgae, while polystyrene nanoparticles functionalized with amino
78 groups (amidine nanoparticles; ANP) can inhibit the growth of microalgae at sufficiently high

79 concentrations (Bergami et al., 2017). Another study showed that algal photosynthesis was
80 hindered by the adsorption of 1.8–6.5 ppm of 20 nm polystyrene nanoparticles, mostly present as
81 aggregates (Bhattacharya, Lin, Turner, & Ke, 2010).

82

83 Heterotrophic bacteria recycle waste and contaminants in marine environments. The water
84 column is full of bacteria in planktonic form, and marine bacteria form biofilms on all available
85 marine surfaces, including ship hulls and the surfaces of marine animals and plants (Dang &
86 Lovell, 2016). Marine bacteria interact with eukaryotic microorganisms such as diatoms to form
87 aggregates called marine snow (Gärdes, Iversen, Grossart, Passow, & Ullrich, 2011), which
88 bring organic carbon and nutrients to the sea floor. Despite the ecological importance of
89 heterotrophic marine bacteria, the impact of plastic nanoparticles on their ecology and
90 physiology is completely unknown.

91

92 Bacteria have been shown to readily attach to and form biofilms on waste plastic in marine
93 environments (Cooksey & Wigglesworth-Cooksey, 1995; Lobelle & Cunliffe, 2011), with
94 different types of plastic selecting for distinct bacterial phyla (Roager & Sonnenschein, 2019). A
95 recent study modeling the effects of biofouling on marine plastics predicted that biofilm
96 formation decreases the onset time of particle settling, as attached organisms weigh down the
97 particles (Kooi, Nes, Scheffer, & Koelmans, 2017). Biofouling of plastic also decreases its
98 hydrophobicity, which can facilitate its passage below the air-water interface of the ocean
99 surface (Lobelle & Cunliffe, 2011). Biofilm formation by marine bacteria on plastic in the
100 oceans could therefore increase the speed with which this plastic makes its way to the sea floor.
101 The effect of plastic nanoparticles on the dynamics of this biofilm formation, however, has not

102 yet been investigated. One study focused on polysaccharides produced by biofouling
103 phytoplankton observed that polystyrene nanoparticles caused an increase in aggregation of
104 polysaccharides (Chen et al., 2011), which suggests that the presence of plastic nanoparticles
105 might stimulate biofilm formation by marine bacteria.

106

107 To test this hypothesis, we investigate the effect of varying concentrations of polystyrene
108 nanoparticles on planktonic growth and biofilm formation of seven species of heterotrophic
109 marine bacteria, both individually and as a community. Marine bacteria were selected to
110 represent a range of biofilm forming abilities. Nanoparticles with two different surface
111 characteristics were selected in order to investigate the potential importance of surface charge
112 and functionality.

113 **Results and Discussion**

114 **Characterisation of nanoparticle and bacteria physical properties**

115 Nanoparticle suspensions of ANPs (Invitrogen™ amidine latex beads, 4% w/v, 0.02 µm; Thermo
116 Fisher catalogue number A37309) and CNPs (Invitrogen™ carboxyl latex beads, 4% w/v, 0.02
117 µm; Thermo Fisher catalogue number C37261) were prepared in both artificial seawater
118 (Millipore Sigma Sea Salts catalogue number S9883, 40 g/L) and marine broth (Bacto Marine
119 Broth, DIFCO 2216). While the individual particles were small (20 nm), ANPs and CNPs
120 exhibited significant aggregation, with dynamic light scattering (DLS) (Zetasizer Nano ZS,
121 Malvern, Massachusetts, USA) indicating that populations of nanoparticles greater than 1 µm
122 existed under all conditions (Figure 1). Additionally, polydispersity indexes (PdIs) were
123 frequently high, suggesting that several populations of aggregate sizes exist within a given
124 suspension. Table 1 lists average size and PDI, together with size distributions. Nanoparticles

125 were characterized in both marine broth, in which experiments were conducted, and artificial
126 seawater, to determine if the characteristics of nanoparticles suspended in nutrient media differed
127 from what could be expected in the open ocean.

128 Broadly, nanoparticles in seawater were aggregated to a larger extent than in broth. This was
129 most pronounced for CNP, with a Z-average diameter of $6,704 \pm 1,746$ nm in seawater, but only
130 202 ± 142 nm in broth (Table 1). Looking at the intensity weighted histograms in Figure 1, this
131 latter value appears to be the average of two distributions, one at 44 nm and the second at
132 approximately 1 μ m. Given that the primary particles are 20 nm, the presence of this smallest
133 peak likely suggests there are a significant fraction of CNP monomers, dimers, and trimers that
134 have been stabilized by organic components of the marine broth. In seawater, this stabilization
135 was not observed, and the smallest detected population occurred at approximately 460 nm. For
136 ANPs, the disparity in Z-average sizes between marine broth and seawater was not as large, and
137 the intensity weighted distributions remain similar.

138 Measurements of zeta potential (an estimate of surface charge) largely followed expected trends
139 in seawater. ANPs were near neutral though slightly positive (2.1 ± 5.4 mV), while the CNPs
140 were more negatively charged (-21.7 ± 5.8 mV). In broth, no significant difference between the
141 zeta potentials of ANPs and CNPs was observed, with all nanoparticles falling between -4.9 and
142 -9.9 mV. This supports the possibility of constituents of the broth adsorbing to the nanoparticle
143 surface, forming a corona, and thereby influencing the surface charge (Fatisson, Quevedo,
144 Wilkinson, & Tufenkji, 2012; Pulido-Reyes, Leganes, Fernández-Piñas, & Rosal, 2017).

145 For tested marine bacteria (Table 2), few differences were observed, with zeta potential falling
146 between -1.7 and -11.1 mV in seawater and marine broth. Under all conditions, the bacteria had a

147 slightly negative charge. The magnitudes of the calculated zeta potential values were all less than
148 ± 30 mV, which is not sufficiently charged to provide a strong barrier to aggregation. As a result,
149 nanoparticle interactions with bacteria would be expected under all conditions.

150 **Impact of nanoplastic on planktonic growth and aggregation of marine bacteria**

151 Neither growth rate nor OD₆₀₀ at stationary phase of tested marine bacteria (Table 2) were
152 impacted by the presence of most tested concentrations of nanoparticles, with the exception of
153 the highest concentration of 200 ppm (Figure 2). At 200 ppm CNP (equivalent to approximately
154 4.5×10^{13} 20 nm particles per mL), *C. marina* exhibited an increased growth rate and OD₆₀₀ at
155 stationary phase, while the maximum optical density attained by *O. kriegii* at stationary phase
156 with this treatment was decreased. The impact of ANPs at the same concentration was more
157 consistent across bacteria, with most species demonstrating a decrease in OD₆₀₀ at stationary
158 phase. Such a decrease can be interpreted either as an increase in aggregation of cells, or as a
159 decrease in total cell numbers due to impaired cell division or cell death.

160 To determine whether the presence of nanoparticles was causing an increase in cell-cell
161 aggregation, we examined the nanoparticle-treated cultures under the microscope after 48 h, and
162 quantified the percentage of total aggregation (Figure 3). Treatment with CNP had little impact
163 on aggregation, with only 200 ppm CNP treatment significantly increasing aggregation of *P.*
164 *carrageenovora* and *C. marina*. In contrast to CNP, treatment with 200 ppm ANP increased
165 aggregation of all bacterial species. Aggregation between negatively charged bacteria might be
166 facilitated by electrostatic interactions with the positively charged amine groups on ANP
167 particles.

168 To determine if treatment with nanoparticles was killing bacterial cells, a dead/live staining assay
169 (BacLight® dead/live stain, ThermoFisher) was conducted on nanoparticle-treated samples after
170 48 h. No impact on the ratio of dead to living cells could be observed up to a nanoparticle
171 concentration of 20 ppm (data not shown). However, fluorescent imaging of planktonic cells was
172 not possible at 200 ppm due to the high concentration of nanoparticles in the suspension. Other
173 studies have observed decreased growth rates of microalgae exposed to polystyrene
174 nanoparticles, although this observation in a photosynthetic organism is most likely due to
175 decreased light penetration caused by high concentrations of nanoparticles in suspension or
176 attached to the cell surface (Baudrimont et al., 2019; Bergami et al., 2017). A study on the
177 marine bacterium *Halomonas alkaliphile* observed that 80 ppm of polystyrene nanoparticles
178 inhibited its growth, which the authors attributed to oxidative stress caused by the generation of
179 intracellular reactive oxygen species (Sun et al., 2018). In the Sun et al. study, it was further
180 observed that positively charged nanoparticles induced higher intracellular levels of reactive
181 oxygen species and thereby oxidative stress than negatively charged ones. This observation
182 offers a possible explanation for why we observed decreased growth in the presence of the
183 neutral/positively charged ANPs but not the more negatively charged CNPs. Most likely, a
184 combination of increased aggregation and decreased growth is responsible for the observed
185 impact of nanoparticles on OD₆₀₀, with the relative contribution of each factor dependent on the
186 bacterial species.

187 **Impact of CNP and ANP on biofilm formation of marine bacteria**

188 Lower concentrations of CNP had no impact on the amount of biofilm formed (Figure 4a). At
189 200 ppm, however, significantly more biofilm was formed by *M. adhaerens*, *M. algicola*, *C.*
190 *marina* and *O. kriegii*. This same concentration of CNP resulted in a small but significant

191 decrease in the amount of biofilm formed by *P. inhibins*. Confocal laser scanning microscopy of
192 biofilms revealed that nanoparticles were integrated into the biofilm itself (Figure 4b),
193 potentially accounting for the increase in total biomass revealed by crystal violet staining.
194 However, *P. inhibins*, which showed a decrease in total biomass with CNP treatment, also
195 integrated CNP into the biofilm. Treatment with 200 ppm CNP had no impact on the ratio of
196 living (green) to dead (red) cells present in any of the biofilms, suggesting the presence of CNP
197 does not kill the cells. Thus, even though the fluorescently-labeled CNP used in the biofilm
198 experiments were not washed to remove any additives present in the stock suspension (Pikuda,
199 Xu, Berk, & Tufenkji, 2018), those additives remaining did not impact cell viability.

200 Lower concentrations of ANP had no impact on the amount of biofilm formed (Figure 5). At 200
201 ppm, however, significantly less biofilm was formed by *M. hydrocarbonoclasticus*, *P. inhibins*,
202 *P. carrageenova*, *M. algicola*, and *C. marina*. This is in contrast to the impact of CNP, which
203 tended to increase total biofilm amount. Treatment with ANP did increase the amount of biofilm
204 formed by *O. kriegii*.

205 Fluorescently labeled ANP are not commercially available, so the presence of ANP in the
206 biofilm could not be assessed using fluorescence microscopy. The ratio of living (green) to dead
207 (red) cells in the ANP treated vs untreated biofilms (Figure 5b) suggests that the presence of
208 ANP did not kill the cells.

209 Concentrations less than 20 ppm of either type of polystyrene nanoparticle had no detectable
210 impact on growth or biofilm formation of the seven tested marine bacteria. This raises the
211 important question of environmentally relevant concentrations. Although it is possible to detect
212 the presence of sub-micron plastic particles in environmental samples using pyrolysis GC-MS

213 (Ter Halle et al., 2017), the confounding influence of other environmental components currently
214 hinders the direct quantification of plastic nanoparticles in environmental samples. In contrast to
215 nanoplastics, microplastics (100 nm - 5 mm) have been well quantified in various marine
216 environments, with the highest concentrations recorded in beach sediments (Besseling, Redondo-
217 Hasselerharm, Foekema, & Koelmans, 2019). As this plastic degrades into nanoparticles, it can
218 be assumed that the highest concentrations of nanoparticles will be achieved in areas rich in
219 plastic debris with little mixing to the wider environment. For example, in sheltered
220 microenvironments of the Great Pacific Garbage patch where plastic is exposed to the degrading
221 effects of photooxidation and mechanical abrasion, and in beach sediments where plastic debris
222 accumulates. To achieve a concentration of 200 ppm, 200 µg of plastic would need to fragment
223 into approximately 4.5×10^{13} nanoparticles contained within 1 mL of seawater. While this does
224 not sound unreasonable within localized microenvironments, the true concentrations of plastic
225 nanoparticles in the environment will remain unknown until technology develops further. The
226 fact that concentrations of less than 20 ppm had no impact on growth or biofilm formation of
227 marine bacteria in our study suggests that plastic nanoparticles present in well mixed pelagic
228 marine environments will most likely not have a significant impact on the formation of marine
229 bacterial biofilms.

230 CNP and ANP had distinctly different impacts on the amount of biofilm formed by the seven
231 tested marine bacteria, presumably due to the unique surface properties imparted by the amidine
232 and carboxyl functionalization. Without control samples treated with non-polystyrene NPs,
233 results of these experiments cannot be attributed to the fact that the NPs are made of polystyrene,
234 but it is clear that surface functionalization of the NPs played an important role. Interestingly, in
235 the presence of ANP, increased cell-cell aggregation was observed in planktonic cultures (Figure

236 3), yet the amount of surface-attached biofilm was decreased (Figure 5). This suggests that
237 nanoparticles in the marine environment might impact pelagic microbial communities differently
238 from sessile ones, although any extrapolations from the experiments performed here to the
239 natural marine environment remain speculative at this point.

240 In the marine broth in which experiments were conducted, CNPs exhibited a large heterogeneity
241 in particle aggregate sizes, with distinct populations clustering around 60 nm and 1100 nm, while
242 ANP clustered exclusively around the 1100 nm range. The size of aggregates formed by the 20
243 nm nanoparticles might therefore be contributing to the observed differences in biofilm
244 formation. When suspended in seawater, CNPs exhibited increased aggregation and lacked the
245 smaller 60 nm population observed in marine broth. This highlights the importance of
246 environmental factors on the behavior of plastic nanoparticles. Previous studies have shown that
247 aggregation of nanoparticles is to be expected under the high-salt conditions of both
248 natural/artificial seawater and marine broth (Alimi et al., 2018; Gigault et al., 2016; Koelmans et
249 al., 2015; Summers et al., 2018). Our experiments were conducted in marine broth in which the
250 surface charge of ANPs particles was decreased, possibly decreasing the impact of surface
251 charge in our experiments compared to what might be expected in natural marine environments.
252 This may at least partially explain why ANPs, which could be expected to facilitate electrostatic
253 interactions between negatively charged bacterial cells and increase cell-cell interactions,
254 actually decreased biofilm formation in most species, rather than increasing it.

255 **Impact of nanoplastic on bacterial community structure**

256 An artificial community was created by combining all seven marine bacteria used in this study
257 (Table 2). The relative abundance of the seven species changed between the three treatments
258 (Figure 6a), with the relative abundance of *M. hydrocarbonoclastic* increasing with nanoparticle

259 treatment, and the relative abundance of *P. inhibins* decreasing. nMDS analysis showed that the
260 species abundance patterns of replicate samples of untreated, CNP treated, and ANP treated
261 biofilms were similar to each other, but significantly dissimilar from other treatments, with no
262 overlap of 95% confidence ellipses (Figure 6b). Presence of either CNP or ANP therefore had a
263 significant impact on the community structure of biofilms, in a reproducible manner that was
264 unique to the nanoparticle type. Although starting communities were identical, the relative
265 abundance of the species comprising the resulting biofilm community that formed in the
266 presence of CNP was significantly different from the relative abundances in the presence of
267 ANP. These results suggest that not only the presence but also the type of nanoparticle can have
268 a significant impact on the biofilm community structure. Interestingly, the specific impacts on
269 community structure could not have been predicted from the results of monoculture experiments.
270 For example, in the presence of ANPs, *M. hydrocarbonoclasticus* dominated the resulting
271 biofilm community. Yet, when a monoculture of *M. hydrocarbonoclasticus* was exposed to
272 ANPs, the amount of biofilm decreased. This suggests that the impacts of plastic nanoparticles
273 on community structure depend not only on physical characteristics of the particles and the
274 bacteria, or on environmental parameters, but also on the interactions between species.
275 Considering our artificial community was composed of only seven species, interactions between
276 species in the natural marine environment can be expected to be even more complex.

277 An additional factor that was not investigated here is the substrate on which the biofilm forms.
278 How the presence of plastic nanoparticles impacts biofilm formation on a plastic substrate is not
279 necessarily indicative of how cell-cell aggregation in a particle of marine snow would be
280 impacted, or how a biofilm would form on the rough surface of a clam shell. The potentially
281 different impacts on free-floating aggregates such as marine snow and sessile marine biofilms is

282 well illustrated by our results showing that ANPs increased aggregation of planktonic bacterial
283 cells (Figure 3), yet decreased surface-attached biofilm formation (Figure 5).

284 **Conclusions**

285 The fact that concentrations of less than 20 ppm had no impact on growth or biofilm formation
286 of marine bacteria in our study suggests that plastic nanoparticles present in well mixed pelagic
287 marine environments will most likely not have a significant impact on the formation of marine
288 bacterial biofilms. Whether lower concentrations might nevertheless impact the community
289 composition of biofilms remains to be determined. The results of our study demonstrate that
290 nanoparticle surface characteristics and concentration both have an impact on biofilm formation
291 by marine bacteria, albeit in a species-specific manner. The impact of plastic nanoparticles will
292 differ between bacterial species, and become increasingly complex as the number of species
293 increases. In order to understand how naturally occurring nanoparticles will impact marine
294 microbial communities, it will be critical to understand the physical properties of naturally
295 produced nanoparticles in the environment.

296 **Acknowledgements**

297 The authors acknowledge the Canada Foundation for Innovation, the Canada Research Chairs
298 program, and the Natural Sciences and Engineering Research Council of Canada (NSERC) for
299 supporting this research. MO was supported by a postdoctoral fellowship from NSERC. We are
300 grateful to the Advanced Bioimaging Facility at McGill University for making the Zeiss 800
301 confocal laser scanning microscope available to us.

302 Tables and Figures Captions

303

304 Table 1. Size and zeta potential of nanoparticles and bacteria used in this study, suspended in
 305 seawater or marine broth. CNPs and ANPs were obtained suspended in water by the
 306 manufacturer without any additives or preservatives. Dynamic light scattering (DLS) was
 307 performed to assess the aggregate size of nanoparticles suspended in artificial seawater or marine
 308 broth media at a particle concentration of 200 ppm. Size measurements are reported as both
 309 intensity-weighted and Z-average (cumulants fit) diameters. The heterogeneity in aggregate sizes
 310 within a suspension is indicated by the polydispersity index (PdI), which ranges from 0 to 1, with
 311 more polydisperse samples approaching unity. Electrophoretic mobility (EPM) measurements
 312 were collected via laser Doppler velocimetry and converted to zeta potential (ZP), providing an
 313 estimate of surface charge which gives insight into the stability of particles in suspension.

314

	Seawater					Marine Broth				
	Z- average Size (d.nm)			Zeta Potential (mV)		Z-average Size (d.nm)			Zeta Potential (mV)	
	avg	std	PdI	avg	std	avg	std	PdI	avg	std
CNP	6704	1746	0.36	-21.7	5.8	202	143	0.83	-9.9	4.6
ANP	2910	1731	0.83	2.1	5.4	1019	104	0.20	-6.6	5.1
<i>M. adhaerens</i>				-6.0	2.3				-8.9	1.4
<i>O. kriegii</i>				-6.7	4.8				-8.8	2.2
<i>M. algicola</i>				-6.5	1.2				-8.1	1.6
<i>C. marina</i>				-10.8	1.2				-9.7	1.1
<i>M. hydrocarbonoclasticus</i>				-6.3	2.6				-9.7	1.6
<i>P. carrageenovora</i>				-7.5	1.8				-11.1	3.2
<i>P. inhibens</i>				-1.7	3.8				-5.6	1.4

315

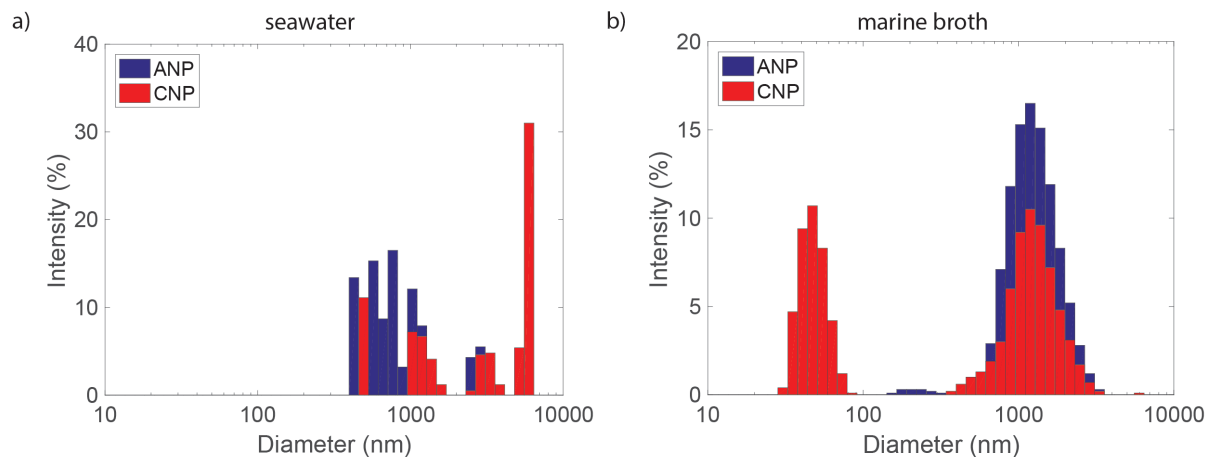
316 Table 2. **Marine biofilm-forming bacteria used in this study.** Strains are ordered by increasing
 317 biofilm-forming ability. All bacterial strains used in this study were obtained from the German
 318 Collection of Microorganisms and Cell Cultures GmbH (DSMZ).

319

	bacterium	Original isolation source	Biofilm formation in this study
1	<i>Marinobacter adhaerens</i> DSM-23420	marine aggregates (0.1-1 mm in diameter) from surface waters, Wadden Sea (Germany)	poor
2	<i>Oceanobacter kriegii</i> DSM-6294 (ATCC 27133)	seawater (USA)	poor
3	<i>Marinobacter algicola</i> DSM-16394	lab culture of dinoflagellate <i>Gymnodinium catenatum</i> YC499B15 (Scotland)	good
4	<i>Cobetia marina</i> DSM-4741 (ATCC 25374)	seawater	good
5	<i>Marinobacter hydrocarbonoclasticus</i> DSM-11845 (ATCC 700491)	oil producing well (Vietnam)	good
6	<i>Pseudoalteromonas carrageenovora</i> DSM-6820 (ATCC 43555)	sample of seawater and marine algae (Halifax, Canada)	excellent
7	<i>Phaeobacter inhibens</i> DSM-17395	seawater from larval cultures of scallop, <i>Pecten maximus</i> (Spain)	excellent

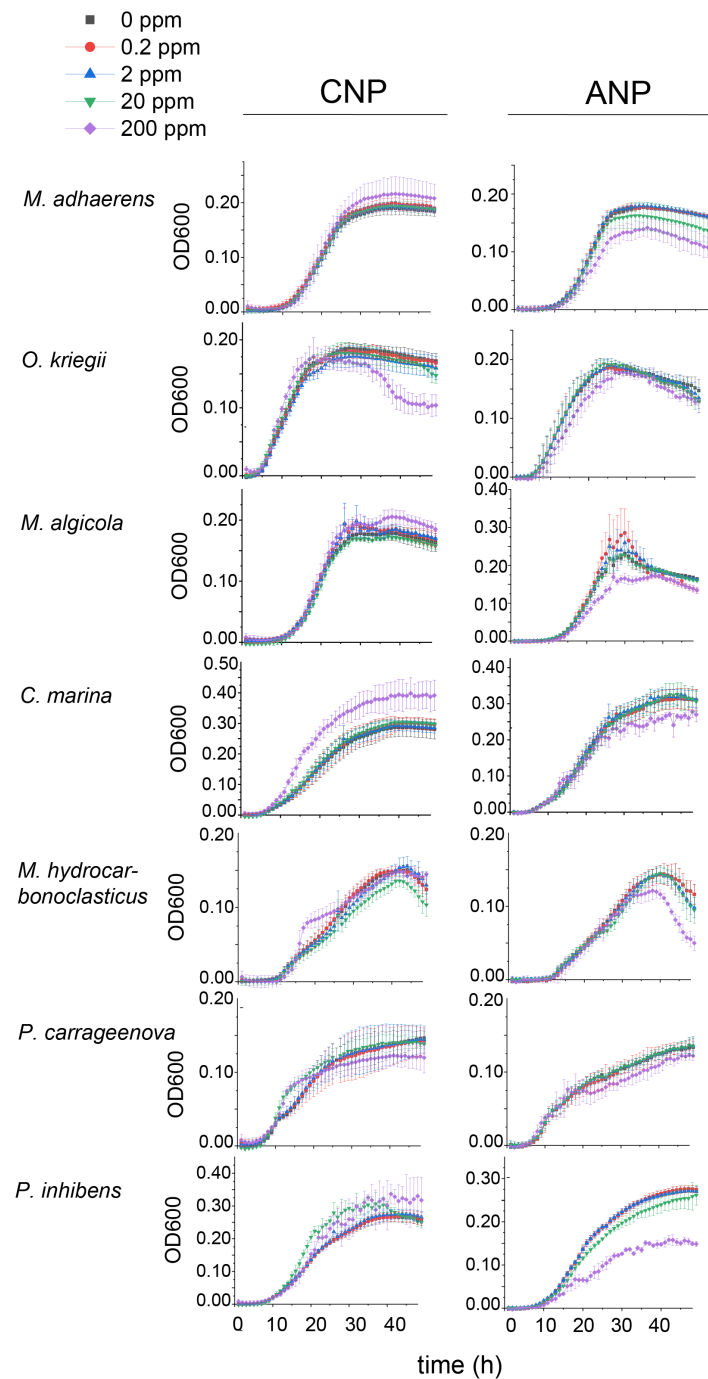
320

321



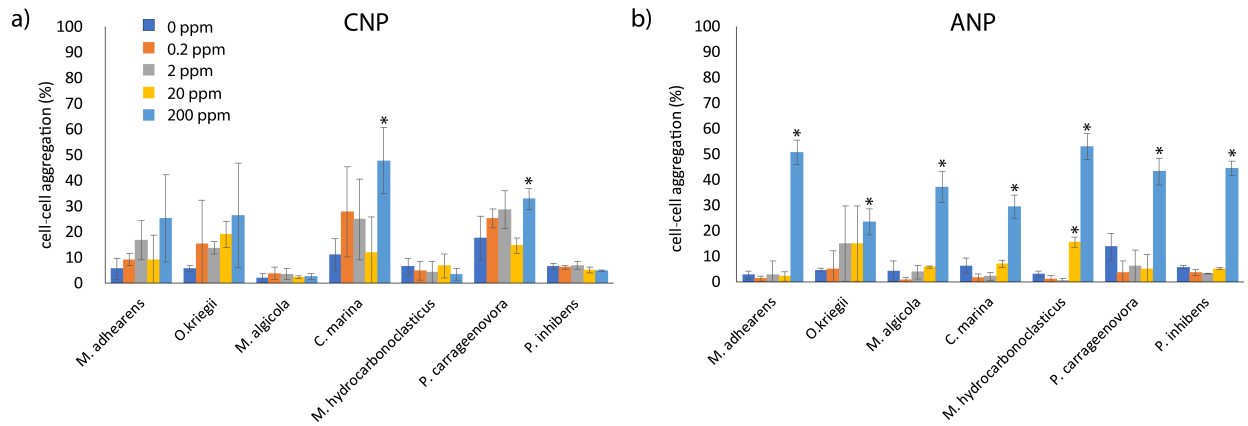
322

323 Figure 1. **Size distribution of 20 nm nanoparticle suspensions** in a) artificial seawater or b)
324 marine broth. Nanoparticles were suspended at a concentration of 200 ppm and corresponding
325 aggregate sizes were determined by DLS. The details of these and all other methods can be found
326 in supplementary data.



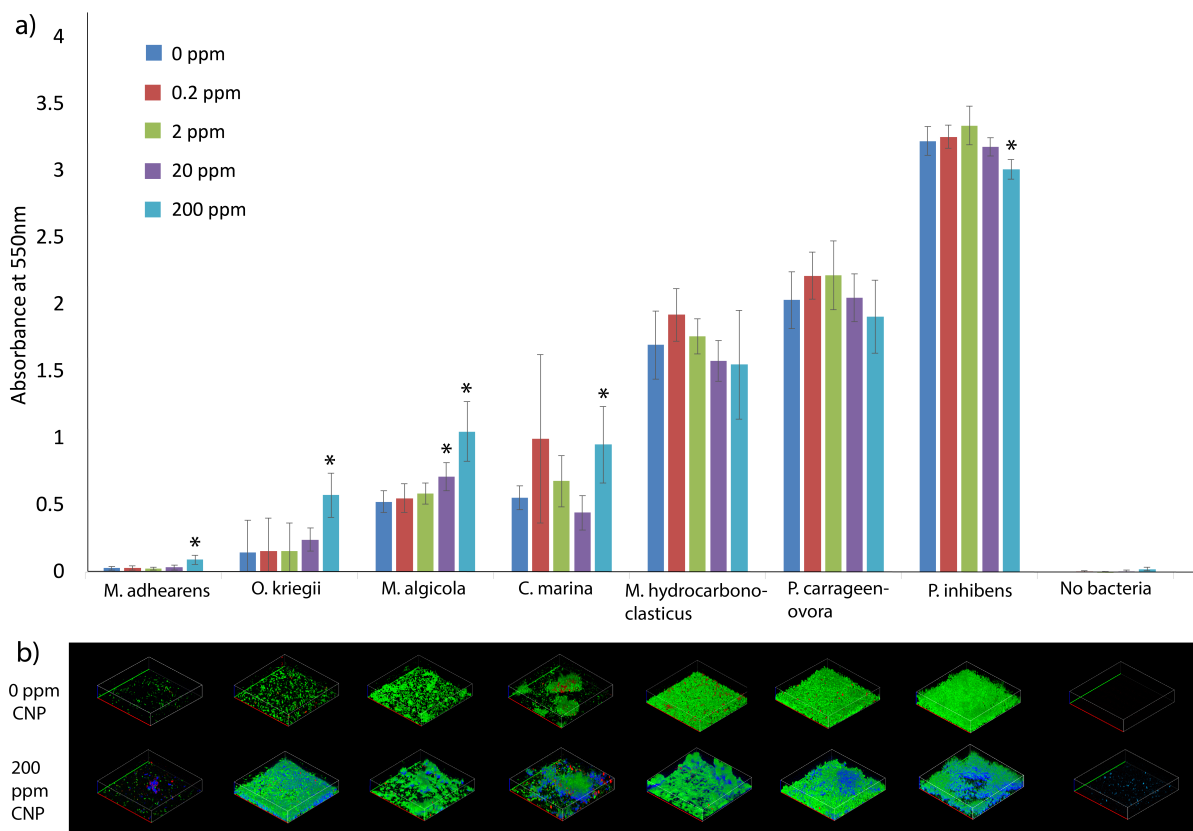
328

329 **Figure 2. Planktonic growth curves in the presence of CNP or ANP.** Bacterial strains were
 330 grown in a 96-well flat-bottom microtitre plate (Costar) over a period of 48 hours in marine broth
 331 containing concentrations of 0, 0.2, 2, 20 or 200 ppm of NPs. Growth curves were repeated three
 332 times and the average value at each time point is reported with error bars showing standard
 333 deviation. OD₆₀₀ was recorded using a Tecan Infinite M200 Pro microplate reader (Tecan Group
 334 Ltd., Switzerland) with 30 s of shaking prior to OD measurement. Optical density of wells with
 335 nanoparticles but no bacteria were subtracted from all wells with bacteria.



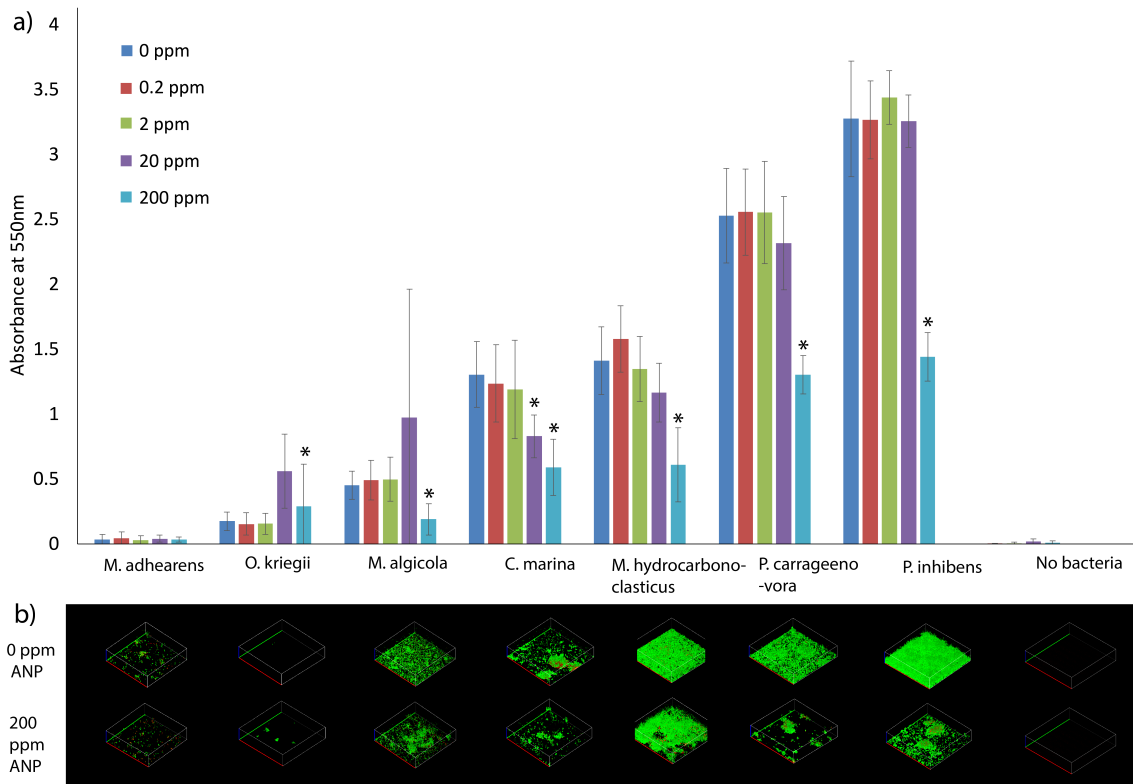
336

337 **Figure 3. Percent aggregation of marine bacteria** in the presence of a) CNP or b) ANP after 48
 338 h of incubation. Bacteria were grown in microfuge tubes on a shaking table at 180 rpm and at room
 339 temperature. Samples were viewed under a compound light microscope at 600× total
 340 magnification. Four independent randomly chosen fields of view were imaged and analyzed using
 341 ImageJ. All groupings larger than 60 pixels² (representing approx. 4 bacterial cells) were
 342 designated as aggregates. Area of aggregated cells was divided by total biomass area to determine
 343 percentage of aggregated biomass. Reported values are the average of four measurements with
 344 error bars showing standard deviation. Values significantly different ($p \leq 0.01$; Student's t-test)
 345 from 0 ppm treatment are indicated by an asterisk.



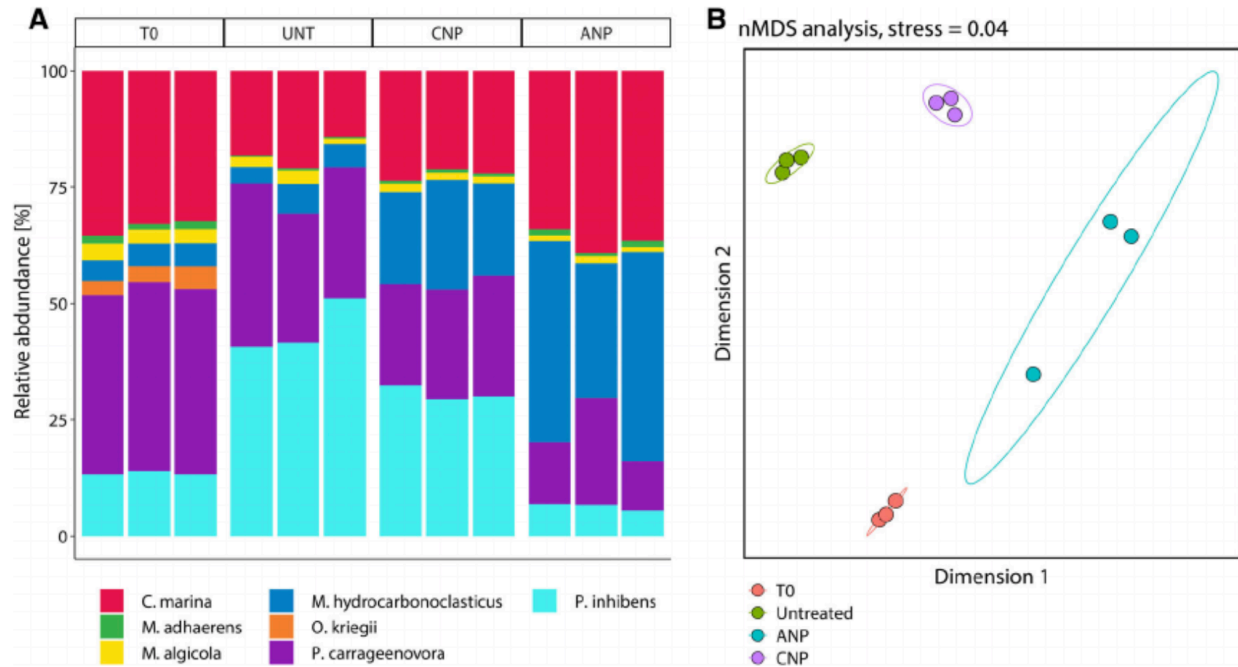
346

347 **Figure 4. Impact of CNP on bacterial biofilm formation.** a) Quantification of biofilm biomass
 348 after five days of incubation by crystal violet staining as per (O'Toole, 2011). Each bar shows the
 349 average of three replicates and error bars show standard deviation. Significant differences ($p \leq$
 350 0.05; Student's t-test) in biomass compared to untreated (0 ppm) are indicated by an asterisk. b)
 351 Representative confocal laser scanning images of untreated biofilms and biofilms grown in the
 352 presence of 200 ppm CNP with blue fluorescence (FluoSpheres® carboxyl-modified microsphere,
 353 0.2 μm , blue fluorescence, 2% solids; ThermoFisher catalogue number F8805). Living cells are
 354 shown in green (stained with SYTO60) and dead cells (defined as compromised membrane
 355 integrity; stained with TOTO-1) are shown in red. Nanoparticles are shown in blue. The length of
 356 red and green axes is 100 μm and the blue axis is 30 μm . Biofilms were imaged in uncoated 96-
 357 well microscopy plates (Ibidi) and using a Zeiss LSM800 confocal laser scanning microscope
 358 equipped with a 63 \times objective. Images were processed using Zen software version 2.3 (Zeiss),
 359 with 3D images rendered using a mixed surface projection.



360

361 **Figure 5. Impact of ANP on bacterial biofilm formation.** a) Quantification of biofilm biomass
 362 after five days of incubation by crystal violet staining (O'Toole, 2011). Each bar shows the average
 363 of three replicates and error bars show standard deviation. Significant differences ($p \leq 0.05$;
 364 Student's t-test) in biomass compared to untreated (0 ppm) are indicated by an asterisk. b)
 365 Representative confocal laser scanning images of untreated biofilms and biofilms grown in the
 366 presence of 200 ppm ANPs. Fluorescent 20 nm ANPs were not available from any commercial
 367 manufacturer and could therefore not be used in this experiment. ANPs are thus present but not
 368 visible in the 200 ppm ANP images. Living cells are shown in green and dead cells (defined as
 369 compromised membrane integrity) are shown in red. The length of red and green axes is 100 μm
 370 and the blue axis is 30 μm . Fluorescent staining and imaging was performed as described for Figure
 371 4B.



372

373 **Figure 6. Impact of CNP and ANP on an artificial biofilm community of marine bacteria.** a)
 374 Relative abundance of seven bacterial species prior to incubation (T0) and community structure of
 375 the biofilm after 5 days incubation in the presence of no nanoparticles (untreated; UNT), CNP, or
 376 ANP. Bacterial species were grown at room temperature on polypropylene squares (0.3 × 0.3 mm)
 377 in marine broth in the presence of 200 ppm ANPs or CNPs. Relative abundances of community
 378 members were determined by 16S rDNA amplicon sequencing with primer set 515f/806R
 379 (Caporaso et al., 2011) and using an Illumina MiSeq. Obtained sequencing read counts were
 380 corrected by the number of the rRNA operons of the respective community members. b) Non-
 381 metric multidimensional scaling (nMDS) of the same communities based on the community
 382 dissimilarity metric ϕ (Quinn, Richardson, Lovell, & Crowley, 2017). nMDS was carried out as
 383 implemented in the R package vegan (Dixon, 2003). Confidence ellipses (95 % level) were
 384 calculated using the R package ellipse (<https://cran.r-project.org/web/packages/ellipse/>) and
 385 assuming a multivariate normal distribution. Relative abundances and the nMDS plot were
 386 visualized using the R package ggplot2 (Wickham, 2016).

387 **References**

388

389 Al-Sid-Cheikh, M., Rowland, S. J., Stevenson, K., Rouleau, C., Henry, T. B., & Thompson, R. C. (2018).
390 Uptake, Whole-body distribution, and depuration of nanoplastics by the scallop pecten maximus
391 at environmentally realistic concentrations. *Environmental science & technology*, 52(24), 14480-
392 14486.

393 Alimi, O. S., Farnier Budarz, J., Hernandez, L. M., & Tufenkji, N. (2018). Microplastics and nanoplastics in
394 aquatic environments: aggregation, deposition, and enhanced contaminant transport.
395 *Environmental science & technology*, 52(4), 1704-1724.

396 Andrady, A. L. (2011). Microplastics in the marine environment. *Marine Pollution Bulletin*, 62(8), 1596-
397 1605.

398 Auta, H., Emenike, C., & Fauziah, S. (2017). Distribution and importance of microplastics in the marine
399 environment: a review of the sources, fate, effects, and potential solutions. *Environment*
400 *international*, 102, 165-176.

401 Baudrimont, M., Arini, A., Guégan, C., Venel, Z., Gigault, J., Pedrono, B., . . . Feurtet-Mazel, A. (2019).
402 Ecotoxicity of polyethylene nanoplastics from the North Atlantic oceanic gyre on freshwater and
403 marine organisms (microalgae and filter-feeding bivalves). *Environmental Science and Pollution*
404 *Research*, 1-10.

405 Bergami, E., Pugnali, S., Vannuccini, M. L., Manfra, L., Faleri, C., Savorelli, F., . . . Corsi, I. (2017). Long-
406 term toxicity of surface-charged polystyrene nanoplastics to marine planktonic species
407 *Dunaliella tertiolecta* and *Artemia franciscana*. *Aquatic Toxicology*, 189, 159-169.
408 doi:<https://doi.org/10.1016/j.aquatox.2017.06.008>

409 Besseling, E., Redondo-Hasselerharm, P., Foekema, E. M., & Koelmans, A. A. (2019). Quantifying
410 ecological risks of aquatic micro-and nanoplastic. *Critical Reviews in Environmental Science and*
411 *Technology*, 49(1), 32-80.

412 Bhattacharya, P., Lin, S., Turner, J. P., & Ke, P. C. (2010). Physical adsorption of charged plastic
413 nanoparticles affects algal photosynthesis. *The Journal of Physical Chemistry C*, 114(39), 16556-
414 16561.

415 Caporaso, J. G., Lauber, C. L., Walters, W. A., Berg-Lyons, D., Lozupone, C. A., Turnbaugh, P. J., . . . Knight,
416 R. (2011). Global patterns of 16S rRNA diversity at a depth of millions of sequences per sample.
417 *Proceedings of the National Academy of Sciences*, 108(Supplement 1), 4516-4522.

418 Chen, C.-S., Anaya, J. M., Zhang, S., Spurgin, J., Chuang, C.-Y., Xu, C., . . . Chin, W.-C. (2011). Effects of
419 Engineered Nanoparticles on the Assembly of Exopolymeric Substances from Phytoplankton.
420 *PLOS ONE*, 6(7), e21865. doi:10.1371/journal.pone.0021865

421 Cooksey, K. E., & Wigglesworth-Cooksey, B. (1995). Adhesion of bacteria and diatoms to surfaces in the
422 sea: a review. *Aquatic Microbial Ecology*, 09(1), 87-96.

423 Cooper, D. A., & Corcoran, P. L. (2010). Effects of mechanical and chemical processes on the degradation
424 of plastic beach debris on the island of Kauai, Hawaii. *Marine Pollution Bulletin*, 60(5), 650-654.

425 Corcoran, P. L., Biesinger, M. C., & Grifi, M. (2009). Plastics and beaches: a degrading relationship.
426 *Marine Pollution Bulletin*, 58(1), 80-84.

427 Dang, H., & Lovell, C. R. (2016). Microbial surface colonization and biofilm development in marine
428 environments. *Microbiol. Mol. Biol. Rev.*, 80(1), 91-138.

429 Dawson, A. L., Kawaguchi, S., King, C. K., Townsend, K. A., King, R., Huston, W. M., & Nash, S. M. B.
430 (2018). Turning microplastics into nanoplastics through digestive fragmentation by Antarctic
431 krill. *Nature communications*, 9(1), 1001.

432 Dixon, P. (2003). VEGAN, a package of R functions for community ecology. *Journal of Vegetation Science*,
433 14(6), 927-930.

434 Fatissou, J., Quevedo, I. R., Wilkinson, K. J., & Tufenkji, N. (2012). Physicochemical characterization of
435 engineered nanoparticles under physiological conditions: effect of culture media components
436 and particle surface coating. *Colloids and Surfaces B: Biointerfaces*, 91, 198-204.

437 Gärdes, A., Iversen, M. H., Grossart, H.-P., Passow, U., & Ullrich, M. S. (2011). Diatom-associated bacteria
438 are required for aggregation of *Thalassiosira weissflogii*. *The ISME journal*, 5(3), 436.

439 Gigault, J., Pedrono, B., Maxit, B., & Ter Halle, A. (2016). Marine plastic litter: the unanalyzed nano-
440 fraction. *Environmental Science: Nano*, 3(2), 346-350.

441 Hernandez, L. M., Xu, E. G., Larsson, H. C., Tahara, R., Maisuria, V. B., & Tufenkji, N. (2019). Plastic
442 teabags release billions of microparticles and nanoparticles into tea. *Environmental science &*
443 *technology*, 53(21), 12300-12310.

444 Hüffer, T., Weniger, A.-K., & Hofmann, T. (2018). Sorption of organic compounds by aged polystyrene
445 microplastic particles. *Environmental pollution*, 236, 218-225.

446 Jambeck, J. R., Geyer, R., Wilcox, C., Siegler, T. R., Perryman, M., Andrady, A., . . . Law, K. L. (2015). Plastic
447 waste inputs from land into the ocean. *Science*, 347(6223), 768-771.

448 Koelmans, A. A., Besseling, E., & Shim, W. J. (2015). Nanoplastics in the aquatic environment. Critical
449 review *Marine anthropogenic litter* (pp. 325-340): Springer, Cham.

450 Kooi, M., Nes, E. H. v., Scheffer, M., & Koelmans, A. A. (2017). Ups and Downs in the Ocean: Effects of
451 Biofouling on Vertical Transport of Microplastics. *Environmental Science & Technology*, 51(14),
452 7963-7971. doi:10.1021/acs.est.6b04702

453 Lambert, S., & Wagner, M. (2016). Characterisation of nanoplastics during the degradation of
454 polystyrene. *Chemosphere*, 145, 265-268.
455 doi:<https://doi.org/10.1016/j.chemosphere.2015.11.078>

456 Lobelle, D., & Cunliffe, M. (2011). Early microbial biofilm formation on marine plastic debris. *Marine*
457 *Pollution Bulletin*, 62(1), 197-200. doi:<http://dx.doi.org/10.1016/j.marpolbul.2010.10.013>

458 Moore, C. J., Lattin, G., & Zellers, A. (2011). Quantity and type of plastic debris flowing from two urban
459 rivers to coastal waters and beaches of Southern California. *Revista de Gestão Costeira*
460 *Integrada-Journal of Integrated Coastal Zone Management*, 11(1), 65-73.

461 O'Toole, G. A. (2011). Microtiter dish biofilm formation assay. *Journal of visualized experiments:*
462 *JoVE*(47).

463 Pikuda, O., Xu, E. G., Berk, D., & Tufenkji, N. (2018). Toxicity Assessments of Micro-and Nanoplastics Can
464 Be Confounded by Preservatives in Commercial Formulations. *Environmental Science &*
465 *Technology Letters*, 6(1), 21-25.

466 Pulido-Reyes, G., Leganes, F., Fernández-Piñas, F., & Rosal, R. (2017). Bio-nano interface and
467 environment: A critical review. *Environmental Toxicology and Chemistry*, 36(12), 3181-3193.

468 Quinn, T. P., Richardson, M. F., Lovell, D., & Crowley, T. M. (2017). propr: An R-package for identifying
469 proportionally abundant features using compositional data analysis. *Scientific reports*, 7(1),
470 16252.

471 Roager, L., & Sonnenschein, E. C. (2019). Bacterial Candidates for Colonization and Degradation of
472 Marine Plastic Debris. *Environmental science & technology*. doi:10.1021/acs.est.9b02212

473 Shim, W., Song, Y., Hong, S., Jang, M., Han, G., & Jung, S. (2014). *Producing fragmented micro-and nano-*
474 *sized expanded polystyrene particles with an accelerated mechanical abrasion experiment*. Paper
475 presented at the 24th Europe SETAC annual meeting, Basel, Switzerland.

476 Summers, S., Henry, T., & Gutierrez, T. (2018). Agglomeration of nano-and microplastic particles in
477 seawater by autochthonous and de novo-produced sources of exopolymeric substances. *Marine*
478 *Pollution Bulletin*, 130, 258-267.

479 Sun, X., Chen, B., Li, Q., Liu, N., Xia, B., Zhu, L., & Qu, K. (2018). Toxicities of polystyrene nano-and
480 microplastics toward marine bacterium *Halomonas alkaliphila*. *Science of the Total Environment*,
481 *642*, 1378-1385.

482 Ter Halle, A., Jeanneau, L., Martignac, M., Jardé, E., Pedrono, B., Brach, L., & Gigault, J. (2017).
483 Nanoplastic in the North Atlantic Subtropical Gyre. *Environmental Science & Technology*.

484 Ward, J. E., & Kach, D. J. (2009). Marine aggregates facilitate ingestion of nanoparticles by suspension-
485 feeding bivalves. *Marine Environmental Research*, *68*(3), 137-142.

486 Wickham, H. (2016). *ggplot2: elegant graphics for data analysis*: Springer.

487 Yousif, E., & Haddad, R. (2013). Photodegradation and photostabilization of polymers, especially
488 polystyrene. *SpringerPlus*, *2*(1), 398.

489